LOW VELOCITY IMPACT ASSESSMENT OF KEVLAR/FLAX-EPOXY COMPOSITE USING IR THERMOGRAPHY

Sy, B.[1], Bougherara, H.[2*], Fawaz, Z.[1*], and Sarwar, A.[2]
[1] Department of Aerospace Engineering, Ryerson University, Toronto, Canada
[2] Department of Mechanical Engineering, Ryerson University, Toronto, Canada
* Corresponding authors (habiba.bougherara@ryerson.ca, zfawaz@ryerson.ca)

Keywords: *Kevlar/Flax; Low Velocity Impact, Infrared Thermography*

ABSTRACT

The use of natural fibers as composite reinforcement has seen a growing interest among both scientists and manufacturers, because of their sustainability, biodegradability, low cost, and relatively high specific properties compared to traditional fibers such as glass. Their usage, however, is mostly limited to non-structural applications because of their weaker mechanical properties and unsatisfactory impact performance compared to most synthetic fibers. One approach for improving their properties while maintaining some cost-benefit and environmental gains is through hybridization with a stronger, stiffer and tougher fibers like aramid. In this study, a hybridized Kevlar® 49/flax-epoxy composite with stacking sequence of $[0_{K2}/0_{F6}]_S$ and $[0_{K2}/(0/90)_{3F}]_S$ is fabricated and tested under 4.5 J, 9 J and 13 J low velocity impact. Passive Infra-Red (IR) thermography is used to monitor the material damage evolution during the impact event. The impact response of the material is characterized in terms of energy absorbed, damaged area, dent depth and thermal response. The results of the analysis show the absorbed energy increasing with impact energy. At the low energy level of 4.5 J, the damage to the samples is attributed to matrix deformation and cracking as exhibited by a small ΔT from the IR recordings. At the higher energy levels of 9 J and 13 J, the damage to the specimen becomes more prominent, manifesting itself through matrix cracks and delamination visible from the back face. Thermographic images show the damage to be mostly in the form of fiber breakage and delamination, with the unidirectional specimens having crack propagation normal to the flax fibers and the cross ply specimens in both longitudinal and transverse directions. For both specimens, the fiber breakage did not propagate all the way through the Kevlar fibers, suggesting the effectiveness of Kevlar fibers in improving the impact toughness of flax-epoxy composites at these energy levels.

1 INTRODUCTION

The use of lignocellulosic natural fibers as reinforcement in a composite structure is not new. In fact, history has shown that this material has been used by multiple civilizations as a means to enhance the stiffness and strength of a particular material or structure. Nowadays, a renewed interest in natural fibers has emerged as an alternative to conventional reinforcement material such as glass fibers. Recent push for sustainability and recyclability have forced industries to find an alternative and ecofriendly materials to produce compatible composites [1,2].

Natural fibers have attracted the interest of both scientists and manufacturers because of their sustainability, biodegradability, abundance, lower cost and lower specific gravity compared to conventional synthetic fibers [1,3]. Although their strengths are relatively lower than synthetic fibers, they have comparable specific properties (i.e.

specific strength and specific stiffness) [4], and acceptable mechanical characteristics such as elongation, flexural strength, impact resistance, non-abrasiveness and acoustic absorption [3]. Despite its great benefits, however, there are still some major drawbacks which restrict its usage in several engineering applications. Compared to synthetic fibers, natural fibers have higher moisture absorption (which makes them incompatible to hydrophobic matrices), and low degradation temperatures (typically below 200°C) which makes them incompatible to high-temperature curing thermosets [3,4,5]. They also exhibit poor fire resistance, susceptibility to microbe infection [3,4], large variability of mechanical properties [5] and poor resistance to weathering [3]. In terms of geometry, natural fibers are also not uniform monofilament cylinders unlike carbon and glass fibers; instead, they are bundles of elementary fibres that contain voids and defects with irregular cross sections [6].

Among the natural fibers, flax is one of the most widely utilized natural fibers because it offers the best potential combination of low cost, light weight and high strength and stiffness for structural applications [5]. In fact, it widely used in the European automotive industry [7] as a thermoplastic composite reinforcement to a car's internal structures for increased strength and impact performance [8,9]. It is a cost-effective material which has the potential to replace glass fibers for a similar application [6]. Moreover compared to glass-epoxy composites, flax-epoxy composites exhibit good damping properties due to its non-linear behaviour when loaded in tension [10,11]. This non-linearity creates a hysteresis loop in the stress strain curve, allowing energy to be dissipated during the loading/unloading process. This is a desirable property especially in sports equipment where vibrational damping is often required [10].

A major drawback with flax fibers is its variability in its properties when exposed to different environmental conditions. Like most lignocellulosic fibers, flax fibers are hydrophilic. Not only it is incompatible with hydrophobic matrices, but it also makes it susceptible to tensile properties degradation with increasing relative humidity [5,6]. Treating the flax fibers with suitable coupling agents such as an alkali or silane treatment will reduce the fiber's moisture absorption capacity and improve fiber-matrix adhesion [5,6,8,11]. It will also enhance the its mechanical and flexural properties [5,6]; however at the expense of a reduction in impact performance [6,11].

A common approach for increasing the mechanical and impact performance of natural fibers is through hybridization with a stronger, stiffer and tougher synthetic fibers such as aramid. The advantage of using a hybrid composite is that one type of fiber can compensate for the disadvantages of the other fiber [10]. In this research, flax and aramid (Kevlar® 49) fibers are hybridized in an attempt to improve the impact performance of flax. Aramid fibers are known for their high tensile strength and stiffness, low density, good impact resistance and damage tolerance [13]. The hybridization of both fibers could potentially create a material with excellent specific strength, stiffness and damping ability, while also offering improved impact strength and toughness. This will be beneficial in automotive and sports equipment applications, where such properties are desirable.

The aim of the present work is to characterize the impact performance of the hybridized Kevlar-Flax fiber-reinforced polymer composite under low velocity/low-energy impact loading. The test will be performed using an in-house designed pendulum-type impact apparatus. The impact performance of the material will be characterized in terms of the energy absorbed, damage mechanism and size. Additionally, an Infra-Red (IR) camera will be used to monitor the thermal response of the material during the impact event. This method will provide valuable information to the damage evolution on the laminate under an impact event, based on the fact that the energy released from any form of damage (matrix cracking, delamination, fiber breakage, etc.) is dissipated as heat. This heat dissipation will be captured by the IR camera as a hot spot on the material surface [14]. Few studies [14,15,16,17] have demonstrated the capability of this method in providing information regarding the initiation and propagation of impact damage.

2 MATERIALS AND TEST METHOD

2.1 Specimen Preparation

A hybrid Kevlar/Flax composite is manufactured from 12 layers commercially available dry UD FlaxPly® fabric (Lineo NV, Belgium), sandwiched in between four layers of DuPont Kevlar® 49 (BGF Industries) woven fabric. For the matrix, an Araldite® LY 565 (epoxy) + Aradur ® 22962 (polyamine hardener) thermosetting resin system is used. This particular resin system has a maximum curing temperature of 150°C, which is below the degradation temperature of the flax fibers. An epoxy-to-hardener ratio of 100:25 parts by weight was used as per the supplier's recommendation. Two 305 mm × 305 mm (12 in. × 12 in.) laminate configurations were manufactured: a unidirectional flax laminate with stacking sequence $[0_{K2}/0_{F6}]_S$ and a cross ply laminate with stacking sequence $[0_{K2}/(0/90)_{3F}]_S$, where the subscript K stands for Kevlar and F for Flax.

The laminate is fabricated using a wet hand lay-up process followed by a compression molding process. For the curing cycle, the plates were initially heated from room temperature to 150°C at 2.5 bars pressure for 0.5 h. This is followed by a steady curing stage for 2.5 h at 150°C/5 bars, and a cooling stage from 150°C to room temperature for another 1 h while maintaining 5 bars pressure [18]. This curing cycle was selected based on a previous work [18] utilizing the same materials and laminate configuration (except that glass fibers were used instead of Kevlar 49). Based on several trials and errors in changing the manufacturing parameters (time, pressure and temperature), this curing cycle produced a laminate with a fiber volume fraction of 50-60% and an acceptable void content of ≤ 3% [18]. The samples were cut into four 152 mm × 152 mm (6 in. × 6 in.) for impact testing.

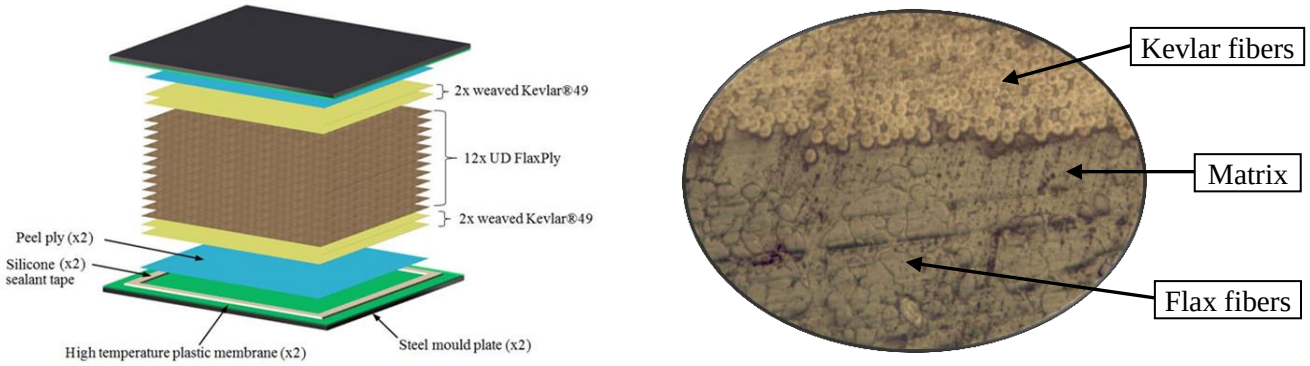

Figure 1. Kevlar/Flax-epoxy laminate assembly (left); Optical micrograph of the unidirectional Kevlar/Flax cross section

2.2 Mechanical Properties

Below are the basic mechanical properties of the composite. The tensile properties were obtained using tensile tests per ASTM D3039 and the flexure modulus was obtained using three-point bending test per ASTM D790.

Stacking Sequence	Thickness (mm)	Density (g/cm^3)	Elastic Modulus E_L (GPa)	Poisson's Ratio, ν_{LT}	Flexure Modulus (Gpa)	Ultimate Tensile Strength (MPa)
$[0_{K2}/0_{F6}]_S$	3.4	1.306±0.026	29.53±2.45	0.342±0.01	19.19±0.40	312.94±4.56
$[0_{K2}/(0/90)_{3F}]_S$	3.4	1.306±0.026	21.44±0.68	0.125±0.03	17.12±0.42	239.11±7.29

Table 1. Basic physical and mechanical properties of Kevlar/Flax-epoxy laminate

2.3 Impact Apparatus

The impact tests were conducted using an in-house designed pendulum impact apparatus. The impact specimen is clamped onto a rigid support fixture with a 127 mm × 127 mm (5 in. × 5 in.) window lodge. The specimen is subjected to an out-of-plane concentrated impact loading at the center of the specimen, using a 4.4 kg steel impactor with a 16 mm diameter steel hemispherical striker tip. This testing effectively simulates the drop-weight impact test per ASTM D7136, except that the impact event is achieved through a swinging pendulum mechanism. To minimize friction and provide free rotation for the pendulum arm, a well-greased ball bearing is used.

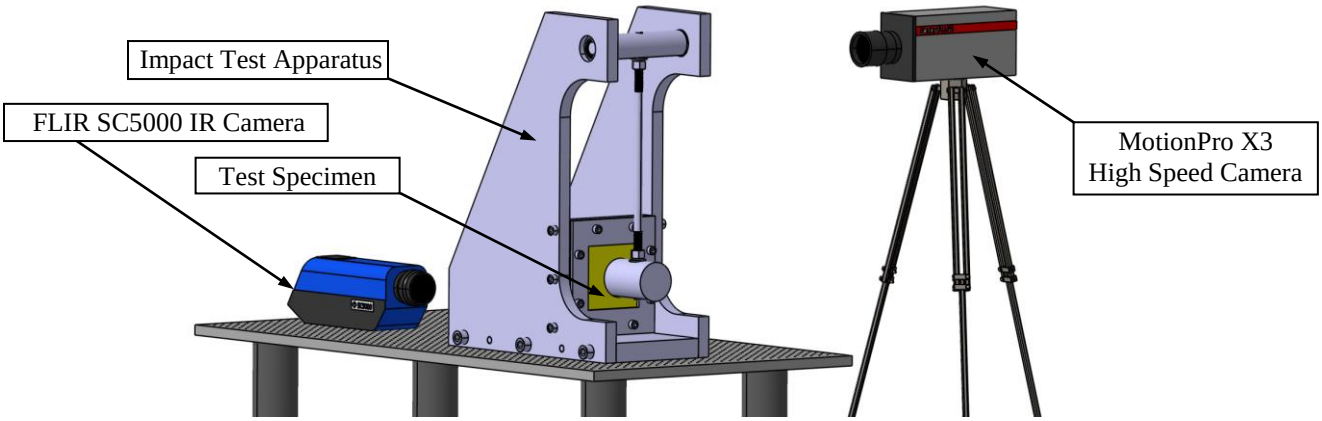

Figure 2. Low Velocity Pendulum Impact Test Setup

The fixture is equipped with two light gates that are positioned along the path of the striker tip such that as the striker approached the specimen, the striker tip blocked gate 1 first and then gate 2 just prior to impact. The actual impact velocity is calculated using the measured times each light gate is obstructed by the striker tip, and the distance between the two light gates. Using the impact velocity, the incident impact energy can be calculated. The impact event is recorded using a high speed camera (MotionPro X3) at a frequency of 1000 Hz.

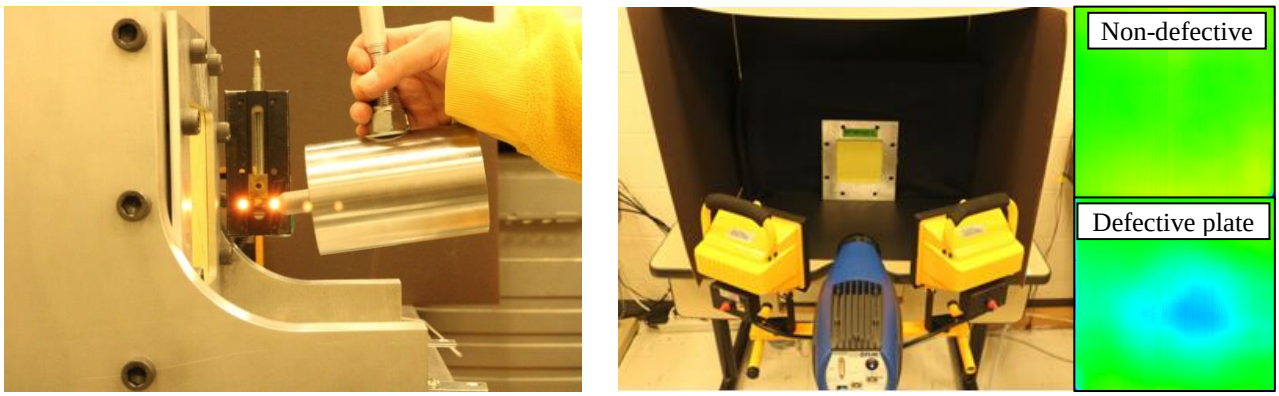

Figure 3. Light gates for velocity measurement (left); Transient thermographic NDT setup (right)

To monitor the specimen's thermal response during the impact event, an IR camera (FLIR SC5000) was positioned at the back side of the specimen (see Figure 2). The camera has a resolution of 320 x 240 pixels and a temperature sensitivity of 20 mK. The impact event was recorded at the maximum camera frequency of 173 Hz.

2.4 Pre-Test Non-Destructive Inspection

Prior to impacting the specimens, the latter were first non-destructively inspected using transient thermographic technique (reflection mode) to search for obvious manufacturing defects (see Figure 3 right). This was performed by briefly heating up the specimen for 20 seconds using two 500W halogen lamps and allowing the specimen to cool down. The heating and cooling down of the specimen is captured using the same IR camera positioned 500 mm in front of the specimen. The presence of defects (e.g. delamination) can be detected as distortion in the temperature field. This distortion is manifested by temperature differences on the material's surface.

2.5 Impact Testing

When a composite specimen is subjected to low velocity impact loading, the total impact energy from the impactor can be categorized as rebound energy ($E_{rebound}$) and absorbed energy ($E_{absorbed}$). The rebound energy comes from the elastic energy stored in the specimen which gets transferred back to the impactor during rebound [19]. The absorbed energy on the other hand is the energy absorbed by the specimen [19] through deformation and the creation of new surfaces through different damage mechanisms [20]. The deformation energy includes the membrane energy E_m and the bending energy E_b, while the damage energy E_d comprises of the energy required to induce matrix cracking, delamination, fiber breakage and fiber pullout.

$$E_{impact} = E_{rebound} + E_{absorbed} \quad (1)$$

where

$$E_{absorbed} = E_m + E_b + E_d \quad (2)$$

The amount of energy absorbed during impact is the difference between the impact energy and the rebound energy.

$$E_{absorbed} = E_{impact} - E_{rebound} \quad (3)$$

From the pendulum impact test, the rebound energy can be determined by calculating the potential energy of the impactor at the recorded rebound height. The remaining energy is the energy absorbed by both the test specimen and the impact test system in the form of heat, vibration, and support reactions [19]. In this study, it is assumed that the energy absorbed by the test system is rather small compared to the energy absorbed by specimen damage and is thus ignored.

In this study, the composite specimens were subjected to incident impact energies of 4.5 J, 9 J and 13 J. Four samples from each configuration were tested for each test case. Each specimen was impacted only once. The required impact energy levels were achieved by adjusting the initial drop height of the pendulum. The elastic energy of the specimen was measured by first recording the maximum rebound angle of the pendulum arm with a high speed camera positioned to the side of the pendulum (see Figure 2). From the rebound angle, the rebound height and energy can be calculated using the potential energy equation. The difference between the total impact energy and rebound energy is the energy absorbed by the specimen, assuming the energy absorbed by the impactor is negligible as indicated earlier.

During the test, the impact response of the Kevlar/Flax-epoxy composite was characterized in terms of the energy absorbed during impact, damage size, dent depth, thermal response and damage evolution during the impact process.

3 RESULTS AND DISCUSSION

3.1 Impact Response

The following figures plot the impact response of the Kevlar/Flax-epoxy composite in terms of the absorbed energy, maximum change in temperature, damage area, dent depth.

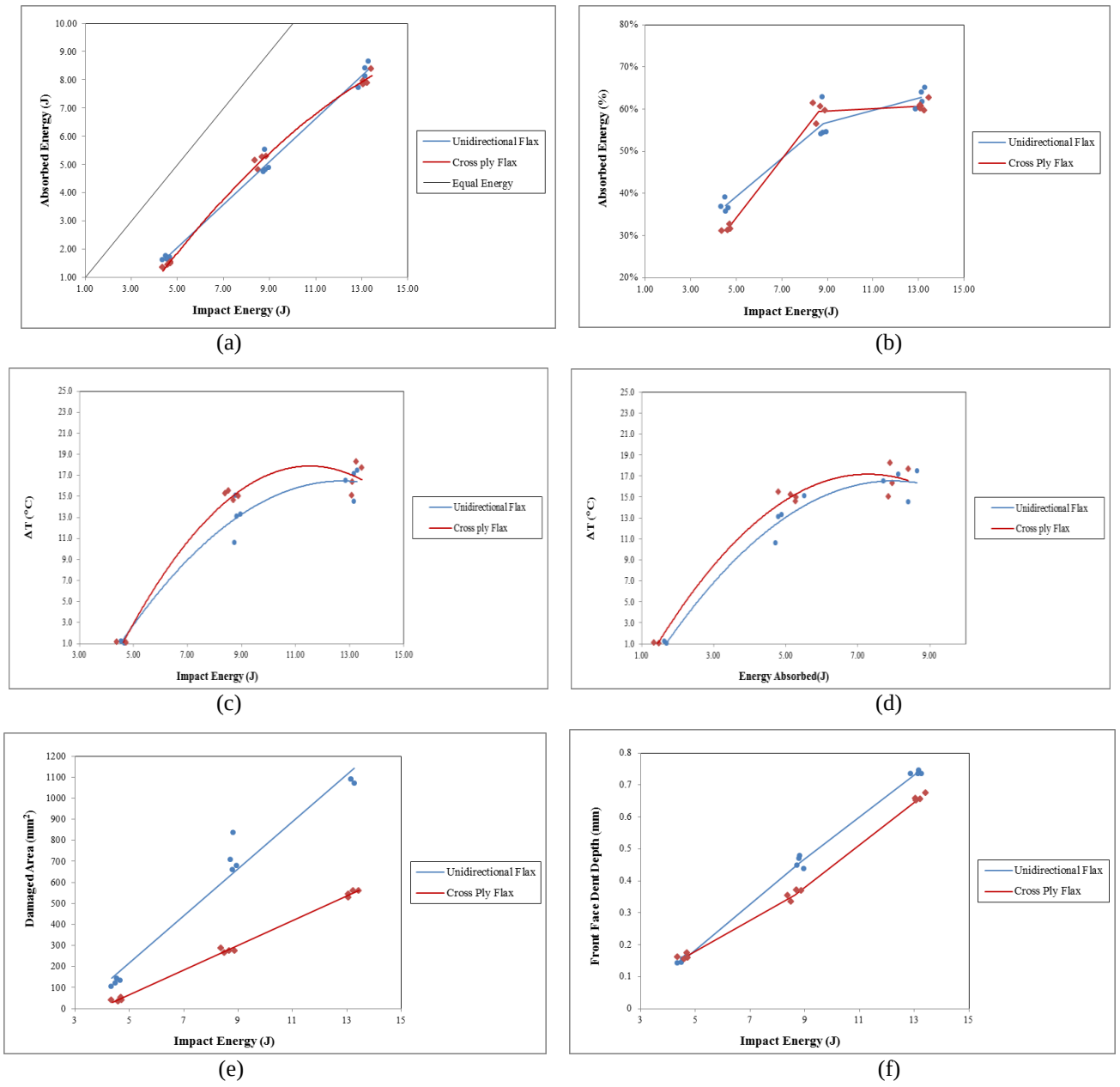

Figure 4. Impact response of the Kevlar-Flax-epoxy composite as a function of impact energy: (a) absorbed energy; (b) absorbed energy percentage; (c) temperature increase (ΔT) ; (d) ΔT vs. $E_{absorbed}$; (e) damaged area; and (f) dent depth

3.2 General Impact Response

The energy absorption characteristic of a composite is typically described in terms of absorbed vs. impact energy. From Figure 4(a), it can be observed that the absorbed energy increases with the incident impact energy, with the unidirectional samples showing a linear relationship with R^2 = 0.992, and the cross ply samples a parabolic relationship with R^2 = 0.997. A closer examination of Figure 4(b) shows that at a lower impact energy of 4.5 J, the unidirectional configuration exhibits a higher energy absorbing capability compared to the cross ply configuration. At a slightly higher energy level of 9 J, the unidirectional configuration shows slightly lower absorbed energy. At 13 J, the difference is not noticeable. This trend can be attributed to the evolution of material damage during an impact event. For all energy levels, all data points are found to be well below the equal energy line, meaning that the penetration threshold was not reached and a large amount of energy is transferred back to rebound the impactor.

Looking at the impact energy vs. percent absorbed energy in Figure 4(b) and the impact energy vs. ΔT in Figure 4(c), the material response can be categorized into three distinct zones. The first zone is at low impact energy levels where the absorbed energy and ΔT is small. This suggests that the damage induced in the material is minor (matrix deformation and cracking), which is also substantiated by the small damaged area on the back face of the specimen. The second zone is at intermediate energy level (9 J), where there is a significant increase in the absorbed energy (50-60%), accompanied by a significant increase in ΔT. This suggests the creation of new surfaces in the specimen through fiber breakage and delamination, as the energy required to produce such damage is much higher compared to matrix cracking and deformation [20]. The third zone is when the slope of the curve starts to decrease, which is more prominent in the cross ply samples at impacted at 13 J. Compared to the unidirectional samples, the cross ply samples exhibit slightly lower energy absorbed accompanied by a smaller damaged area. This material behavior may be attributed to the change in stiffness of the material due to fracture events.

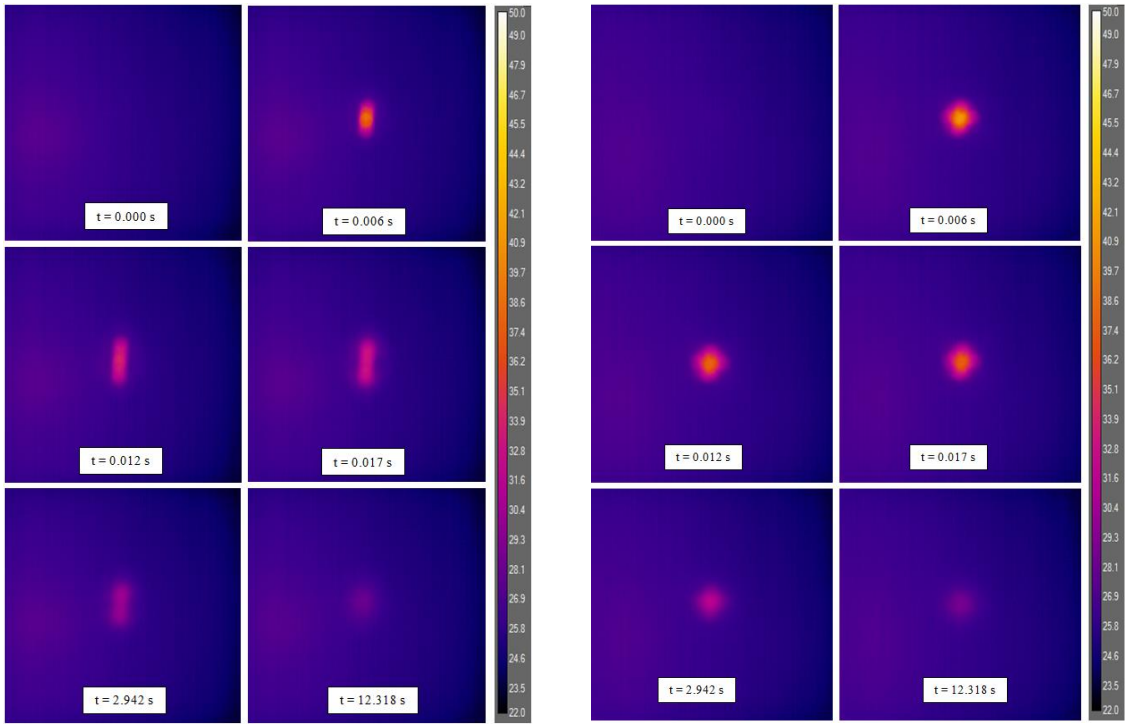

Figure 5. Material damage evolution in unidirectional (left) and cross ply samples (right) at E = 10 J

3.3 Material Damage Evolution

During an impact event, the damage process is initiated by matrix deformation and cracking followed by fracture process. From Figure 5, it can be observed that damage to the composite initiated at the impact point, as evidenced by the circular hot spot (where ΔT is maximum) at the center of impact. For the unidirectional sample, this hot spot extends in the direction normal to the flax fibers, which likely indicates the onset of fiber breakage. At t = 0.017 s, the area of the hot zone expands in the form of an ellipse (with decreasing ΔT), which indicates the formation of a delamination zone. As time progresses, the hot spot cools down towards ambient temperature, however, at a slow rate because of the entrapped heat within the delamination zone. The same behavior can be observed in the cross ply samples, except that the hot spot propagates in both the longitudinal and transverse directions of the specimen.

3.4 Damage Analysis

A visual examination of the back face damage area shows the damage shape of the unidirectional laminate is elliptical with its major axis perpendicular to the flax fiber direction, while the damage area of the cross ply laminate is rhombical/cross-shaped. Thus for the damage area calculation, the damage area for the unidirectional laminate is approximated as an ellipse, while the damaged area for the cross ply is approximated as rhombus. A plot of the damaged area vs. impact energy in Figure 4(e) shows a linear relationship between the damage area and impact energy, with the unidirectional laminates showing larger damaged area compared to the cross ply laminates for the same impact energy. Moreover, the rate of increase in the damage area with impact energy is higher for the unidirectional laminates as compared to that of the cross ply laminates, as indicated by the steeper line gradient.

Figure 6 shows the visual and thermographic (IR) images of the back face area post-impact. For a low impact energy (E_{impact} = 4.5 J), the damage to the back face is minimal and is manifested by slightly whitened area of about few millimeters in diameter. An examination of the thermal images for both the unidirectional and cross ply configurations shows a very small hot spot behind the impact point with a temperature rise of $\Delta T < 2°C$. This small ΔT suggests that the damage mechanism for this impact energy level includes only matrix deformation and some matrix cracking. This behavior is consistent with brittle polymer matrices, where the energy required for matrix deformation and cracking is small [20], which in turn gives rise to a small temperature increase [15]. The ΔT for both configurations is almost of equal magnitude, although the unidirectional samples show slightly larger whitened area as compared to the cross ply sample. This behavior can be attributed to the difference in the flexural stiffness between the two laminates, with the unidirectional laminates being stiffer (thus more brittle) than the cross ply ones.

At higher impact energies (9 J and 13 J), the damage to the back face of the samples becomes more prominent with obvious signs of macro cracks and delamination. The delamination area and crack length also increases with increasing energy level. For the unidirectional samples, the macro-crack propagates in the direction normal to the flax fibers. The IR images show the crack originating at the point of impact where ΔT is at maximum, and propagates normal to the flax fiber direction (ΔT decreasing away from the central hot spot). This transverse crack propagation indicates the occurrence of fiber breakage in the laminate. Surrounding the crack are slightly cooler zones, which may be due to delamination of the outer fiber layers from the matrix. At 9 J impact energy, the crack is only visible in the transverse (90°) direction, indicating that fiber breakage only occurred within the flax-epoxy layers. At 13 J, the crack also started to propagate in the longitudinal direction of the laminate, indicating that the crack has extended into the woven Kevlar layers. This can also been seen from the third IR image in Figure 6(a), as the hot spot starts to extend into the 0° direction of the laminate. It must be noted, however, that although the crack seemed to have extended to the Kevlar layers, the impact energy was not high enough to cause complete breakage

of the Kevlar fibers. For the cross ply laminates, the cracks propagate in both the longitudinal and transverse directions of the laminate, with the crack lengths almost equal in both directions.

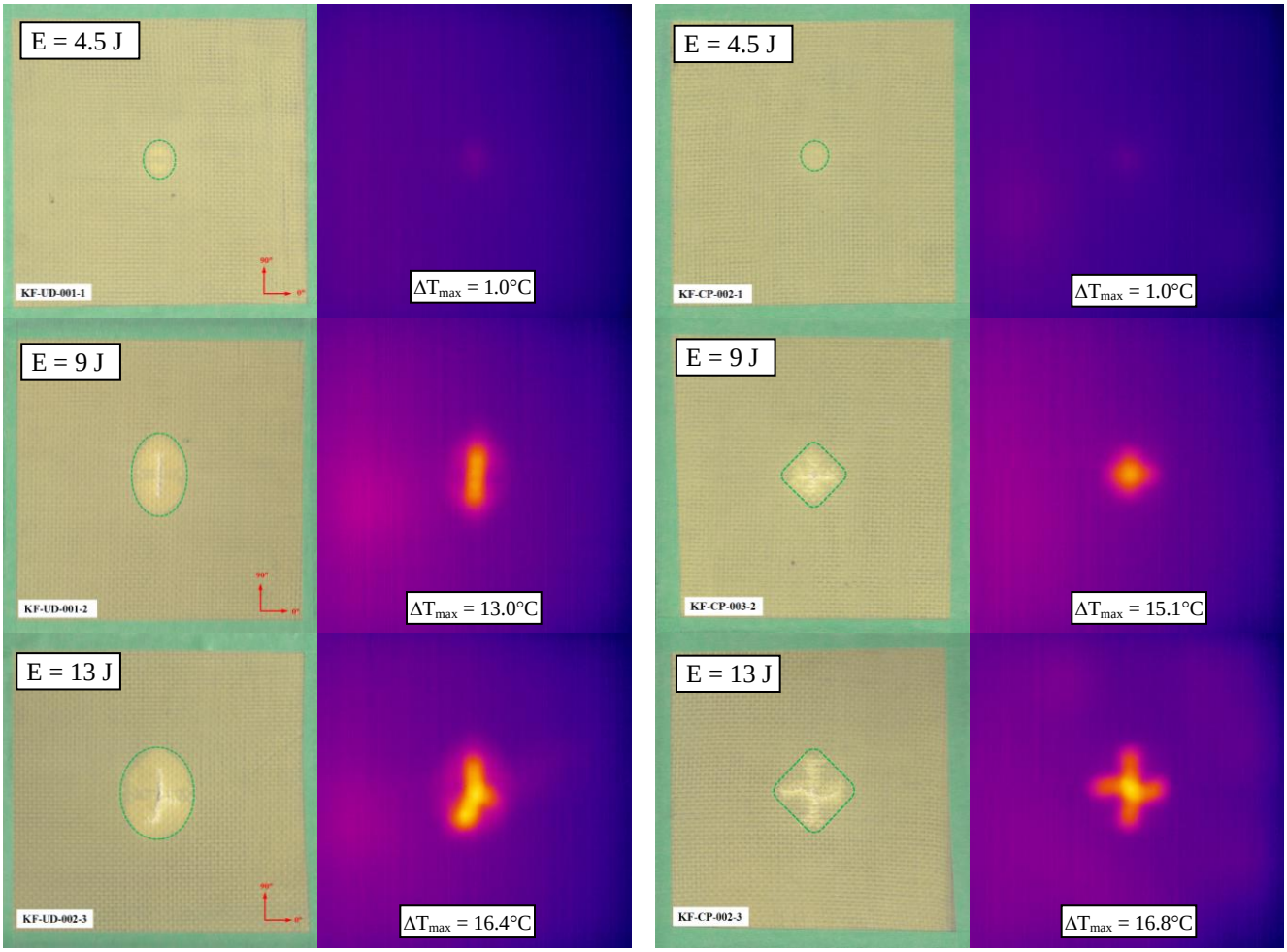

Figure 6. Back face visual damage and corresponding thermal signature for unidirectional (left) and cross ply samples (right)

4 CONCLUSION

In this paper, experimental investigations of the low velocity impact behavior of hybrid Kevlar-Flax-epoxy composite have been conducted using a pendulum-type impact apparatus, with IR thermography to monitor the material damage evolution during the impact event. The results of the analysis show the absorbed energy increasing with impact energy. At a low energy level (4.5 J), the damage to the samples is minimal, most likely in the form of matrix deformation and cracking as exhibited by a small ΔT from the IR recordings. At higher energy levels (9 J and 13 J), the damage to the specimen becomes prominent manifested mostly by matrix cracks and delamination through the back face. Thermographic images show the damage is most likely caused by fiber breakage and delamination, with the unidirectional specimens having crack propagation normal to the flax fiber directions and the cross ply specimens in both longitudinal and transverse directions. For both specimens, the fiber breakage did not propagate all the way through the Kevlar fibers, suggesting that the hybridization with woven Kevlar fibers is

effective in improving the toughness of flax-epoxy composites. Future work in this area includes testing pure flax-epoxy composites under the same impact parameters in order to quantify the improvement in the material's impact toughness as a result of hybridization with Kevlar 49. Impact testing up to penetration will also be conducted to quantify the penetration threshold of the hybrid Kevlar-Flax-epoxy composite material system.

5 REFERENCES

[1] H. Hamada, J. Denault, A.K. Mohanty, Y. Li and M.S. Aly-Hassan. "Natural fiber composites". *Advances in Mechanical Engineering*, Vol. 5, No. 569020, 2013.

[2] E.A. Elbadry, M.S. Aly-Hassan and H. Hamada. "Mechanical properties of natural jute/jute mat fiber reinforced polymer matrix hybrid composites". *Advances in Mechanical Engineeering*, Vol. 4, No. 354547, 2012.

[3] N. Sgriccia, M.C. Hawley, M. Misra. "Characterization of natural fiber surfaces and natural fiber composites". *Composites Part A: Applied Science and Manufacturing*, Vol. 39, No. 10, pp 1632-1637, 2008

[4] F. Ahmad, H. S. Choi, and M.K. Park, "A review: Natural fiber composites selection in view of mechanical, light weight, and economic properties". *Macromolecular Materials and Engineering*, Vol. 300, No. 1, pp. 10–24, 2015.

[5] L. Yan, N. Chouw and K. Jayaraman. "Flax fibre and its composites – a review". *Composites Part B: Engineering*, Vol. 56, pp. 296-317, 2014.

[6] D.B. Dittenber and H. GangRao. "Critical review of recent publications on use of natural composites in infrastructure." *Composites Part A: Applied Science and Manufacturing*, Vol. 43, No.8, pp. 1419-1429, 2012.

[7] M. Karus and M. Kaup. "Natural fibers in the European automotive industry". *Journal of Industrial Hemp*, Vol. 7, No. 1, pp. 119-131, 2002.

[8] J. Summerscales, N. Dissanyake, A.S. Virk and W. Hall. "A review of bast fibres and their composites. Part 1 – fibres as reinforcements". *Composites: Part A*, Vol. 41, pp. 1329-1355, 2010.

[9] S. Kalia, B.S. Kaith and I Kaur. "*Cellulose Fibers: Bio- and Nano-Polymer Composites"*. Springer, 2011.

[10] J. Flynn, A. Amiri and C. Ulven. "Hybridized carbon and flax fiber composites for tailored performance". *Materials and Design*, Vol. 102, pp. 21-29, 2016.

[11] Z. Mahboob, I.E. Sawi, R. Zdero, Z. Fawaz and H. Bougherara. "Tensile and compressive damaged response in flax fibre reinforced epoxy composites". *Composites: Part A*, Vol. 92, pp. 118-133, 2017.

[12] M.A. Fuqua, S. Huo and C.A. Ulven. "Natural fiber reinforced composites". *Polymer Reviews*, Vol. 52, No. 3, pp. 259-320, 2012.

[13] F.C. Campbell. "*Manufacturing Process for Advanced Composites*". Elsvier Ltd., 2004.

[14] C. Meola and G.M. Carlomagno. "Infrared thermography to evaluate impact damage in glass/epoxy with manufacturing defects". *International Journal of Impact Engineering*, Vol.16, pp. 1-11, 2014.

[15] C. Meola and G.M. Carlomagno. "Impact damage in GFRP: New insights with infrared thermography". *Composites: Part A*, Vol. 41, pp. 1839-1847, 2010.

[16] V.P. Vavilov. "Modelling and characterizing impact damage in carbon fiber composites by thermal/infrared non-destructive testing". *Composites: Part B*, Vol. 61, pp. 1-10, 2014.

[17] I.M. De Rosa, C. Santulli, F. Sarasini and M. Valente. "Post-impact damage characterization of bybrid configurations of jute/glass polyester laminates using acoustic emission and IR thermography". *Composites Science and Technology*, Vol. 69, pp. 1142-1150, 2009.

[18] S. Manteghi, Z. Mahboob, Z. Fawaz and H. Bougherara. "Investigation of the mechanical properties and failure modes of hybrid natural fiber composites for potential bone fracture fixation plates". *Journal of the Mechanical Behaviour of Biomedical Materials*, Vol. 65, pp. 306-316, 2017.

[19] T.J. Kang and C. Kim. "Impact energy absorption mechanism of largely deformable composites with different reinforcing structures". *Fibers and Polymers*, Vol. 1, No. 1, pp. 45-54, 2000.

[20] B. Agarwal, L. Broutman and K. Chandrashekhara. "*Analysis and Performance of Fiber Composites*". 3rd edition, Wiley and Sons, Inc., 2006.